Linear Electric Shifts in the Paramagnetic Resonance of Al_2O_3:Cr and MgO:Cr†

E. B. ROYCE* AND N. BLOEMBERGEN
Division of Applied Physics, Harvard University, Cambridge, Massachusetts
(Received 11 April 1963)

It is shown that the spin Hamiltonian for Cr^{3+} ions in the Al_2O_3 lattice has to be augmented by a term $\Sigma_i \Sigma_j \leq_k \frac{1}{2} R_{ijk} E_i (S_j S_k + S_k S_j)$ in the presence of an externally applied electric field **E**. The five independent components of the third rank R tensor appropriate to the point symmetry C_3 of the Cr^{3+} sites have been determined experimentally. In units of Mc/sec per kV/cm the results for one site are $R_{111}=-0.020$, $R_{222}=0.073$, $R_{333}=0.179$, $R_{123}=0.04$, and $R_{113}=0.09$. The Cr^{3+} site in the unit cell related by inversion symmetry has all signs reversed. The two other sites which are related to this pair by a reflection in the y plane have the signs of R_{222} and R_{123} reversed. These results are related to the known crystal structure. Their agreement with a theoretical calculation based on a partially covalent bonding orbital in the CrO_6^{-9} complex is satisfactory, whereas a point-charge model of the crystal field cannot account for the spin Hamiltonian. The electric field effect for the Cr^{3+} sites with an associated vacancy in the MgO lattice, was shown to be less than 1 Mc/sec for $E=10^5$ V/cm, in agreement with the covalent theory. Verification of the Kramers degeneracy in the presence of the crystalline field components of odd parity resulted in setting an upper bound on the permanent electric dipole moment of the electron of 1.4×10^{-15} cm times e.

I. INTRODUCTION

AN applied electric field may induce linear shifts in the paramagnetic resonance line spectrum when paramagnetic ions occupy sites which lack inversion symmetry.[1] The effect was first observed by Ludwig and Woodbury[2] for transition metal impurities in silicon. Artman and Murphy[3] observed linear electric shifts of the $m_s=\pm\frac{3}{2}\rightarrow\pm\frac{1}{2}$ transitions of the Cr^{3+} spins in Al_2O_3, when a magnetic and electric field are applied parallel to the c axis. Recently, similar results[4] have been obtained for Fe^{3+} and Mn^{4+} in Al_2O_3.

It had been pointed out earlier[5] that the angular dependence of the influence of an applied electric field on the spin Hamiltonian is described phenomenologically by tensors of odd rank. The third-rank tensor in C_3 symmetry, appropriate to the Cr^{3+} sites in Al_2O_3, has five independent components. All of these components can be determined experimentally, if the magnetic field is applied at an angle with the trigonal axis so as to mix the m_s states. In Sec. II of this paper experiments are described which determine the electric shift as a function of the directions of the applied magnetic and electric fields. These results have been reported earlier in an abbreviated form.[6]

Since the Al_2O_3 crystal as a whole has inversion symmetry, there is no piezoelectric effect. Electrostrictive effects are quadratic in the electric field strength. Hence, the linear electric shifts are observed at constant strain. Since the Cr^{3+} sites occur in pairs related to each other by inversion symmetry, the Cr^{3+} ions at these sites will experience equal electric shifts in opposite directions. A magnetic resonance line will exhibit an apparent splitting in the applied electric field. A similar pseudo-Stark splitting has been observed for the optical R lines in ruby.[7]

Experiments have also been carried out to detect the linear electric shifts of the paramagnetic resonance lines of Cr^{3+} in MgO with an associated vacancy. No linear effect was observable. Effects quadratic in the electric field strength for paramagnetic impurities in MgO, Al_2O_3, and $KTaO_3$ have been reported by others.[8,9]

In Sec. III of this paper the experimental results will be compared with theoretical calculations of the effects of an applied electric field on the spin Hamiltonian in ruby. The linear electric shift is due, in general, both to a displacement of the positive and negative ions with respect to each other and to a distortion of the electron orbitals at constant internuclear distances. It turns out that the ionic displacement effect is more important. It does not act, however, in a direct manner by a change

† This paper is based on portions of a thesis presented to Harvard University in fulfillment of the thesis requirement for the Ph.D degree (Cruft Laboratory Technical Report TR-379) and has been supported by the Joint Services through the Office of Naval Research Contract 1866(16).

* National Science Foundation predoctoral fellow.

[1] N. Bloembergen, Science **133**, 1363 (1961).

[2] G. W. Ludwig and H. H. Woodbury, Phys. Rev. Letters **7**, 240 (1961); F. S. Ham, *ibid.* **7**, 242 (1961); G. W. Ludwig and F. S. Ham, *ibid.* **8**, 210 (1962); G. W. Ludwig, in Proceedings of the First International Conference on Paramagnetic Resonance, The Hebrew University, Jersalem, Israel, 1962 (to be published).

[3] J. O. Artman and J. C. Murphy, Bull. Am. Phys. Soc. **7**, 14 (1962).

[4] J. J. Krebs, Bull. Am. Phys. Soc. **8**, 259 (1963).

[5] J. A. Armstrong, N. Bloembergen, and D. Gill, Phys. Rev. Letters **7**, 11 (1961).

[6] E. B. Royce and N. Bloembergen, Bull. Am. Phys. Soc. **7**, 200 (1962); N. Bloembergen and E. B. Royce, in Proceedings of the First International Conference on Paramagnetic Resonance, The Hebrew University, Jerusalem, Israel, 1962 (to be published).

[7] W. Kaiser, S. Sugano, and D. L. Wood, Phys. Rev. Letters **6**, 605 (1961); M. D. Sturge and K. A. Ingersoll, Bull. Am. Phys. Soc. **8**, 215 (1963).

[8] M. Weger and E. Feher, in Proceedings of the First International Conference on Paramagnetic Resonance, The Hebrew University, Jerusalem, Israel, 1962 (to be published).

[9] S. H. Wemple, Bull. Am. Phys. Soc. **8**, 62 (1963).

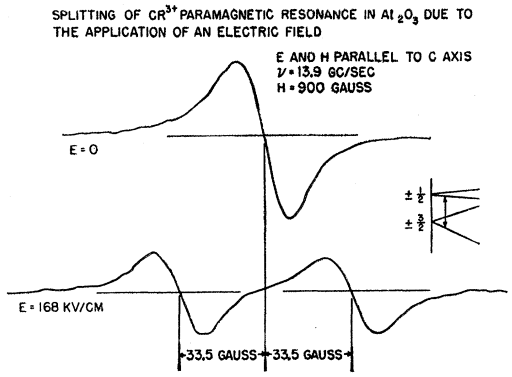

FIG. 1. Experimental absorption derivative curves showing the electric-field-induced splitting of the $\frac{1}{2} \rightarrow \frac{3}{2}$ resonance line of Cr^{3+} in ruby.

in the crystal field potential from displaced point charges. The change in interionic distances produces a fractional change in the partial covalent bonding of the chromium to its ligands and this, in turn, changes the splitting of the spin quartet of the orbital ground state. A simple point-charge model will be shown to be inconsistent with all available data of the spin Hamiltonian.

II. EXPERIMENTAL PROCEDURE AND RESULTS

Ruby samples were cut in the form of platelets $\frac{1}{4}$ mm thick, and evaporated silver electrodes were applied to the samples. With such samples it was impossible to eliminate tangential components of the microwave fields at the electrodes. The electrodes were made much less than one microwave skin depth in thickness in order not to perturb seriously the microwave field. Such electrodes are semitransparent optically but have sufficient direct current conductivity. Fine copper wires were soldered to the sample ultrasonically with indium to provide leads to the electrodes. The sample was then entirely coated with an insulating material to prevent electrical breakdown from one electrode to the other around the edge of the sample.

A rectangular waveguide cavity operating in the TE_{012} mode near 13.9 Gc/sec was used, with the sample located at the center of the cavity at the position of maximum microwave magnetic field. Provision was made for adjusting the tuning and coupling of the cavity remotely. Coupling was adjusted by moving a Teflon wedge into a section of waveguide beyond cutoff, and tuning was adjusted by threading a Teflon rod into the cavity. The electrical leads to the sample electrodes were brought into the cavity through large holes in the sides. The paramagnetic resonance spectrometer used was of the conventional magic tee bridge design, using bolometer detection when saturation was no problem and crystal detection otherwise. The frequency of the Varian X-12 klystron was stabilized at the resonance of the cavity with sample by an FM feedback technique.

Magnetic field modulation and phase-sensitive detection produce a recording of the absorption derivative, when the dc magnetic field is swept through resonance with an without applied electric field. Figure 1 shows the pseudo-Stark splitting of the $m_s = \frac{3}{2} \rightarrow \frac{1}{2}$ transition, when both the electric and magnetic field are applied along the c axis. Examination of the absorption curve in Fig. 1 shows that there is no residual unsplit line at the center of the pattern, that neither split component is appreciably broader than the original resonance line, and that the center of the unsplit line is midway between the centers of the two components. Figure 2 shows the dependence of this splitting on the strength of the applied electric field for several samples. The effect is linear in the applied electric field for splittings greater than one linewidth. Data for individual samples show a scatter of 1% from linearity, though different samples differ by as much as 5% from one to the other. This difference is due to variations in the preparation of the electrodes on the samples, such as the closeness of the plated area to the edge of the sample. The two boules were both Linde ruby, the Cr^{3+} concentration in both being 0.05%. The electric field splitting was also observed in a 0.17% Cr^{3+} sample with no difference being noted. No temperature dependence was observed to liquid-nitrogen temperature.

If the electric field strength is not large enough to produce a resolved splitting, the additional broadening from unresolved splittings may be used. Figure 3 shows that the additional broadening of the same transition at low electric fields is proportional to the square of the electric field strength. The empirical relationship

$$\frac{\text{change in linewidth}}{\text{linewidth}} = (0.90 \pm 0.05)\left(\frac{\text{splitting}}{\text{linewidth}}\right)^2, \quad (1)$$

was used to calculate the splitting from the observed

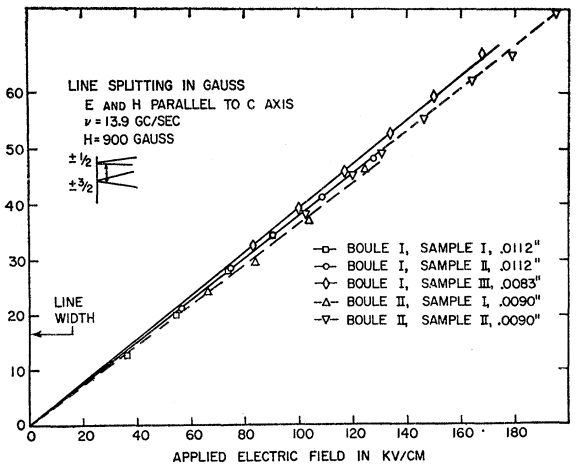

FIG. 2. Linear variation of electric-field-induced line splitting.

unresolved line broadening. This procedure is necessary for other orientations of the crystal with respect to the externally applied fields, since the electric shifts are generally smaller in those circumstances.

Figure 4, taken from a paper by Geschwind and Remeika,[10-12] shows a portion of the structure of ruby. Note that there are four distinct, nonequivalent sites for the chromium ions which replace aluminum ions substitutionally. These sites are indistinguishable in the usual paramagnetic resonance spectrum of chromium, but each site behaves differently under the influence of an applied uniform electric field. Sites b and c in the figure are related to each other by the symmetry operation of inversion through the metal atom, as are f and a. Sites c and a are related by reflection in a vertical mirror plane normal to the y or A axis, as are b and f. The difference between b and c, on the one hand, and f and a, on the other hand, is the result of a 4.3° rotation of one-half of the oxygen triangles forming the local environment of the metal atom, as the figure shows. Since none of the sites is itself an inversion center, the application of a uniform electric field produces a linear shift in the resonance value of the magnetic field for each particular site, and an equal but oppositely directed shift of the resonance field for the site related to the first by the symmetry operation of inversion. If the magnetic field has a component along the y axis the degeneracy of the spectrum for the a and c sites, or the b and f sites, is also lifted by the electric field. In this case the resonance splits into four components.

The angular dependence of this electric field effect was measured by varying the directions of the applied electric and magnetic fields. The electric field induced shift of the energy levels giving rise to the paramagnetic resonance transitions may be described formally by the addition of terms to the spin Hamiltonian describing these levels:

$$\begin{aligned}\mathcal{H}_S=&g_{\parallel}\beta H_zS_z+g_{\perp}\beta(H_xS_x+H_yS_y)\\&+D[S_z^2-\tfrac{1}{3}S(S+1)]\\&+\sum_i\sum_{j\le k}\tfrac{1}{2}R_{ijk}E_i(S_jS_k+S_kS_j)\\&+\sum_{ijk}T_{ijk}E_iH_jS_k. \quad (2)\end{aligned}$$

The first three terms are the usual spin Hamiltonian,[13,14] with $g=1.98$, $D=-5.7$ Gc/sec, $S=\frac{3}{2}$. The term containing the R tensor is a perturbation of D, while the T-tensor term is a perturbation of g. Making use of the C_3 symmetry of the chromium site, it can be shown that these tensors take the forms below, where 1,2,3 refer to x,y,z, respectively.

	S_1^2	S_2^2	S_3^2	$\frac{1}{2}(S_2S_2+S_3S_2)$	$\frac{1}{2}(S_1S_3+S_3S_1)$	$\frac{1}{2}(S_1S_2+S_2S_1)$
E_1	R_{111}	$-R_{111}$	0	R_{123}	R_{113}	$-2R_{222}$
E_2	$-R_{222}$	R_{222}	0	R_{113}	$-R_{123}$	$-2R_{111}$
E_3	R_{311}	R_{311}	R_{333}	0	0	0

(3)

	S_1H_1	S_2H_2	S_3H_3	S_2H_3	S_1H_3	S_1H_2	S_3H_2	S_3H_1	S_2H_1
E_1	T_{111}	$-T_{111}$	0	T_{123}	T_{113}	$-T_{222}$	T_{132}	T_{131}	$-T_{222}$
E_2	$-T_{222}$	T_{222}	0	T_{113}	$-T_{123}$	$-T_{111}$	T_{131}	$-T_{132}$	$-T_{111}$
E_3	T_{311}	T_{311}	T_{333}	0	0	0	0	0	0

(4)

The trace of the perturbation, $\sum_jR_{ijj}$, may be taken equal to zero, in which case one has $R_{311}=-\frac{1}{2}R_{333}$. This gives five independent components in the R tensor. If the trace of the perturbation is not taken equal to zero, there would be six independent components, but one of them could not be evaluated experimentally. The terms may be grouped into three groups, one longitudinal term, two transverse, and two skew terms, according to the orientation of the magnetic field with respect to the c axis of the crystal. The longitudinal term appears with the applied electric and magnetic fields parallel to the c axis and is described by R_{333}. The transverse terms involving R_{111} and R_{222} and the skew terms involving R_{113} and R_{123} occur for a transverse electric field, with the magnetic field transverse or skew to the c axis, respectively. All but the longitudinal term give no first-order contribution to the energy if the magnetic field is parallel to the c axis. A transverse component of the magnetic field is required to mix the states and, thus, to bring in the transverse and skew terms linearly in the perturbation. With the magnetic field parallel to the c axis, there may be, however, a quadratic electric field effect from the transverse and skew components of the R tensor, as can be calculated from second-order perturbation theory on the pure state wave functions. Except for the $\frac{1}{2}\rightarrow-\frac{1}{2}$ transition, this quadratic effect would be in addition to the linear effect from R_{333}. It has been observed on the $\frac{1}{2}\rightarrow-\frac{1}{2}$ transition.[8]

It was found possible to fit all of the experimental results using only the R tensor, and for this reason only

[10] S. Geschwind and J. P. Remeika, Suppl. J. Appl. Phys. **33**, 370 (1962).
[11] H. Winchell, Bull. Geol. Soc. Am. **57**, 295 (1946).
[12] W. G. Wyckoff, *Crystal Structures* (Interscience Publishers, Inc., New York, 1960).
[13] G. M. Zverev and A. M. Prokhorov, Zh. Eksperim. i Teor. Fiz. **34**, 513 (1958) [translation: Soviet Phys.—JETP **7**, 354 (1958)].
[14] J. E. Geusic, Phys. Rev. **102**, 1252 (1956).

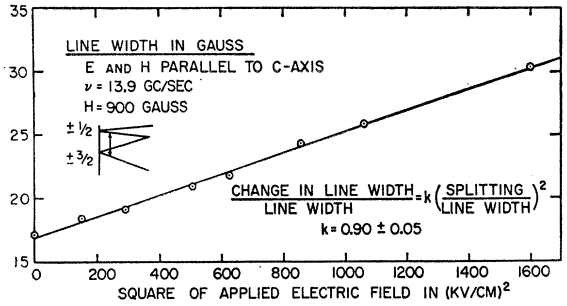

FIG. 3. Quadratic variation of electric-field-induced line broadening for splittings less than one linewidth.

the R tensor is considered in the following analysis. Limits on the values of the components of the T tensor may be estimated from the experimental uncertainties quoted on the values of the components of the R tensor. It is not surprising that the T tensor may be ignored, since g is close to the free spin value and crystalline field effects on g are small.

The usual spin Hamiltonian has been diagonalized by Chang and Siegman[15] for arbitrary angles of the magnetic field with respect to the z axis. Their wave functions,

$$|\rangle = a|\tfrac{3}{2}\rangle + b|\tfrac{1}{2}\rangle + c|-\tfrac{1}{2}\rangle + d|-\tfrac{3}{2}\rangle \qquad (5)$$

were used as a basis set for evaluating the perturbation induced by the electric field. Writing out the perturbation terms in the modified spin Hamiltonian yields

$$\begin{aligned}\mathcal{H}_E' = {} & (R_{111}E_1 - R_{222}E_2)(S_1^2 - S_2^2) \\ & - (R_{222}E_1 + R_{111}E_2)(S_1S_2 + S_2S_1) \\ & + (R_{123}E_1 + R_{113}E_2)\tfrac{1}{2}(S_2S_3 + S_3S_2) \\ & + (R_{113}E_1 - R_{123}E_2)\tfrac{1}{2}(S_1S_3 + S_3S_1) \\ & + \tfrac{3}{2}R_{333}E_3[S_3^2 - \tfrac{1}{3}S(S+1)]. \qquad (6)\end{aligned}$$

Taking diagonal elements of this perturbation between the wave functions given by Chang and Siegman yields

$$\begin{aligned}\mathcal{H}_E' = {} & [(R_{111}E_1 - R_{222}E_2)\cos 2\phi \\ & - (R_{222}E_1 + R_{111}E_2)\sin 2\phi]A(\theta) \\ & + [(R_{113}E_1 - R_{123}E_2)\cos\phi \\ & + (R_{123}E_1 + R_{113}E_2)\sin\phi]B(\theta) \\ & + \tfrac{3}{2}R_{333}E_3C(\theta), \qquad (7)\end{aligned}$$

where

$$\begin{aligned}A(\theta) &= 2\sqrt{3}(bd + ac) \\ B(\theta) &= \sqrt{3}(ab - cd) \qquad (8) \\ C(\theta) &= (a^2 - b^2 - c^2 + d^2).\end{aligned}$$

The dependence of these diagonal elements on the orientation of the electric field is given by the components E_1, E_2, E_3. The Chang and Siegman wave functions assume the magnetic field to lie in the xz plane; ϕ is the azimuthal angle about the z axis of the magnetic field out of this plane. The dependence on the polar angle of the magnetic field from the z axis is contained in the coefficients a,b,c,d, and is not given explicitly.

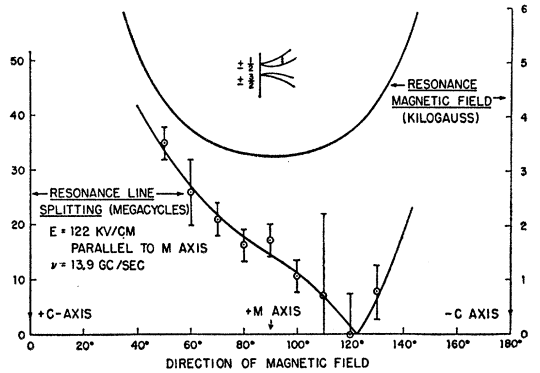

FIG. 5. Angular dependence of electric-field-induced splitting where the magnetic field is rotated about the y axis. E is parallel to the x axis.

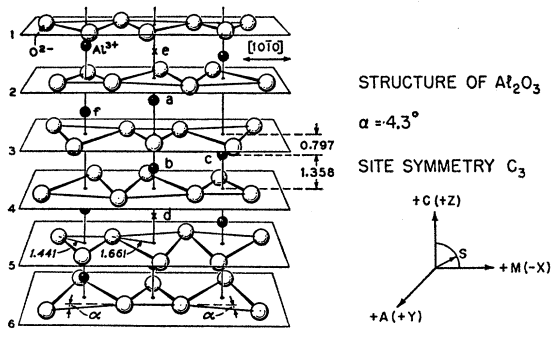

FIG. 4. Portion of the Al_2O_3 lattice showing the coordinate system used in this work. (After Geschwind and Remeika.)

By orienting the electric and magnetic fields along certain selected directions, it was possible to evaluate each component of the R tensor. The linearity with applied electric field for the effect depending on each component of the R tensor was verified at these orientations.

The electric field splitting was measured as a function of the angle of the magnetic field for several directions of the applied electric field. Figure 5 shows the dependence of the splitting induced by E_x on the polar angle Θ of the magnetic field for an azimuthal angle $\phi = 0°$. The curves drawn are the evaluation of the perturbation terms in the modified spin Hamiltonian [Eqs. (7) and (8)]. Values of the components of the R tensor were selected to fit the experimental data. In the particular case shown, the effect comes from mixing the skew component R_{113} and the transverse component R_{111} of the R tensor. The line splits into two rather than four components since for these orientations the four

[15] W. S. Chang and A. E. Siegman, Stanford Electronics Laboratory Technical Report 156-2, reproduced in J. Weber, Rev. Mod. Phys. **31**, 681 (1959).

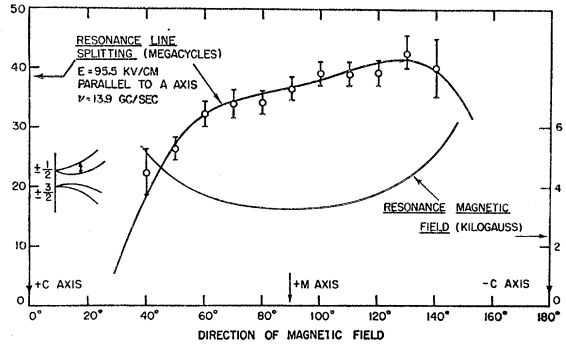

FIG. 6. Angular dependence of the electric-field-induced splitting where the magnetic field is rotated about the y axis. E is parallel to the y axis.

sites are grouped into two sets of equivalent pairs of sites.

Figure 6 shows the dependence on the polar angle of the magnetic field, again for an azimuthal angle of $\phi=0°$, but with the electric field along the y axis. The effect here comes from a mixing of the transverse component R_{222} and the skew component R_{123} and is a splitting into two rather than four components. Relative signs as well as magnitudes of the skew and transverse components were evaluated from such measurements.

Figure 7 shows the dependence of the effective electric field splitting on the azimuthal angle of the magnetic field with a polar angle of $\theta=90°$. Two transverse orientations of the electric field were taken. Only the transverse components of the R tensor R_{111} and R_{222} enter. In this case, there is no equivalence of the two kinds of sites which are mirror images of each other in the y plane. The electric field broadening or splitting is never zero, since the zeros for the splitting for these two sites occur at different angles. The calculated splitting of each kind of site is shown as a dashed line, and the total calculated effective splitting as a solid line. The latter can be shown to be the square root of the sum of the squares of the individual splittings of the two kinds of sites. The contributions from each site were determined by selecting values of the components of the R tensor for each site to best fit the total effective splitting to the experimental points. The relative signs of R_{111} and R_{333} were determined in a measurement on a separate sample, where the electric field was taken at a skew angle to the z axis.

From the symmetrical position of the minimum splitting at zero degrees in Fig. 7, it follows that each site contributes equally and, hence, that the populations of the sites related to each other by reflection symmetry are the same to one part in seven. The absence of a shift in center of gravity and the fact that the intensities of the split components are equal, allows the deduction that the populations of the sites related to each other by inversion are equal to one part in two hundred. We can also say that sites such as d in Fig. 4, which have inversion symmetry, are not populated. Geschwind and Remeika[16] have, by contrast, demonstrated that for gadolinium in Al_2O_3, sites related to each other by reflection in the y plane have unequal populations. These results could be obtained by magnetic resonance without an applied electric field because Gd^{3+} has such a high spin that its resonance shows a variation with the azimuthal direction of the magnetic field. Two differences between these cases should be noted. First, gadolinium is a much worse fit than chromium in the Al_2O_3 lattice due to its larger ionic radius; and second, the chromium doped samples were flame grown, wereas the gadolinium doped samples were grown from a flux. Geschwind and Remeika did not observe site selectivity for iron in flux grown Al_2O_3, and iron has an ionic radius more comparable to chromium.

Table I gives the final best fit for the components of the R tensor taking all kinds of data into account. Relative signs of the various components are significant. The first two sets of data refer to the two kinds of sites related to each other by reflection; the sites related by inversion have all signs reversed. If the coordinate system is rotated by $5°\pm1°$ about the c axis, R_{111} can be made zero. In C_{3v} site symmetry R_{111} would be zero if the x axis is normal to the mirror planes. R_{123} is small in the rotated coordinate system, but does not vanish. The deviation from C_{3v} symmetry is small, but this shows that the local symmetry of the chromium site is truly C_3, since R_{123} would vanish in C_{3v} symmetry. One of the two oxygen triangles making up the local environment of the magnetic ion is aligned with an edge parallel to the original coordinate system, while the second triangle is rotated by 4.3°. This indicated that the effect arises predominantly from this second triangle, for which the Cr-O distance is 10% shorter.

TABLE I. Experimental values of the components of the R tensor for two types of sites in ruby. Units are Mc/sec per kV/cm. Sites related to these by inversion have all signs reversed.

R_{111}	-0.020 ± 0.003	-0.020 ± 0.003
R_{222}	0.073 ± 0.003	-0.073 ± 0.003
R_{333}	0.179 ± 0.003	0.179 ± 0.003
R_{123}	$0.04\ \pm0.02$	$-0.04\ \pm0.02$
R_{113}	$0.09\ \pm0.02$	$0.09\ \pm0.02$
	In a coordinate system rotated by 5°	
R_{111}	0	
R_{222}	0.076 ± 0.003	
R_{333}	0.179 ± 0.003	
R_{123}	$\pm0.04\ \pm0.02$	
R_{113}	$0.09\ \pm0.02$	

The chromium impurity in MgO enters the lattice substitutionally for magnesium, predominantly at sites which have a cubic environment.[17,18] Such a site should

[16] S. Geschwind and J. P. Remeika, Phys. Rev. **122**, 757 (1961).
[17] J. E. Wertz and P. Auzins, Phys. Rev. **106**, 484 (1957).
[18] J. H. E. Griffiths and J. W. Orton, Proc. Phys. Soc. (London) **73**, 948 (1959).

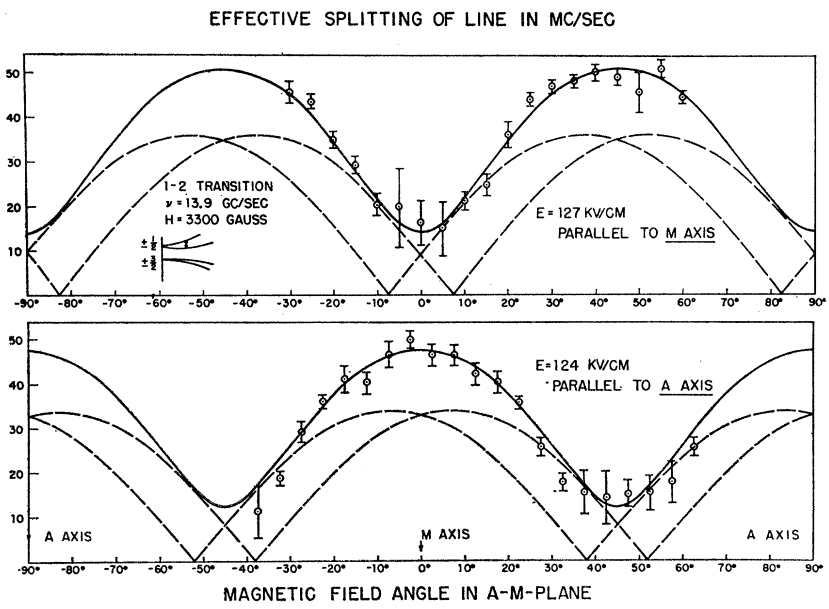

FIG. 7. Angular dependence of the electric-field-induced splitting where the magnetic field is rotated about the z axis. Electric field along the x and y axes, respectively.

be an inversion center and, hence, cannot show a linear electric field effect. A few percent of the chromium ions are found at sites whose spectrum has axial symmetry. It is thought that for these sites there is a magnesium vacancy at the nearest magnesium site along a [100] direction. (MgO has the NaCl structure.)

The energy levels giving rise to the magnetic resonance spectrum for this defect site as well as any possible linear electric field effects will be described by a spin Hamiltonian of the form given for ruby in Eq. (2). For the defect site, one has $|D|=2.5$ Gc/sec and $g=2.00$. For the local site symmetry C_{4v}, the nonzero elements of the R tensor are $R_{113}=R_{223}$ and $R_{333}=2R_{311}=2R_{322}$, where the trace of the perturbation has again been set equal to zero. If the magnetic field is along a [100] direction, it will be in the x, y, or z direction for each third of the sites. The two-thirds of the sites where the field is perpendicular to the z axis give a different spectrum from the one-third where it is parallel. An applied electric field parallel to the magnetic field should produce a linear electric field splitting of the z-axis spectrum, but not the x- and y-axis spectra.

In looking for this small effect, an ac electric field was applied to the sample and phase detection was used. Simultaneous magnetic field modulation was added, and the phase detection took place at the difference frequency between the magnetic modulation frequency and twice the electrical modulation frequency. A small signal was observed on the z-axis spectrum. Unfortunately, a comparable signal was also observed on the x- and y-axis spectra, and it was concluded that these signals were spurious. It was possible only to set an upper bound on the electrically induced broadening, and to set an upper bound on the effective splitting. It was determined that $|R_{333}|$ must be less than 0.01Mc/sec per kV/cm.

III. THEORETICAL CONSIDERATIONS

The fact that one of the two oxygen triangles forming the local environment of the chromium ion dominates the other triangle in producing the electric field effect on the chromium magnetic resonance in ruby indicates that the part of the crystalline field responsible for the electric field effect is of covalent rather than electrostatic origin. An electrostatic interaction of the oxygen ions on the chromium wave functions would not be very different for the ions of the two triangles since the chrome-oxygen distances differ by less than 10% between the two triangles. On the other hand, a covalent interaction could be much more sensitive to distance, and thus be responsible for the electric field effect.

For ruby, one has $R_{333}/D=31\times10^{-6}$ cm/kV, while for the defect site in MgO:Cr, one has $R_{333}/D\leq4\times10^{-6}$ cm/kV. The noncubic part of the crystalline field arises from a next nearest neighbor vacancy in MgO, whereas in ruby, it arises from a distortion of the nearest neighbor symmetry. The large difference in the R_{333}/D ratios, noted above, can be explained readily on the basis of covalent interactions, which should be negligible for next nearest neighbors. These two arguments support the idea that a theory of the electric field effect must take covalent effects into account explicitly.

Artman and Murphy[19] have worked out a theory of the electric field effect in ruby in a crystal field formalism,[20] taking the matrix elements of the crystal field as adjustable parameters. Such an approach to crystal field theory has been successful in interpreting the opti-

[19] J. O. Artman and J. C. Murphy, Bull. Am. Phys. Soc. **7**, 196 (1962); J. O. Artman, in Proceedings of the First International Conference on Paramagnetic Resonance, The Hebrew University, Jerusalem, Israel, 1962 (to be published).

[20] Y. Tanabe and S. Sugano, J. Phys. Soc. Japan **9**, 753, 766 (1954) (I and II).

cal spectrum of ruby.[21–24] Artman and Murphy have pointed out that crystal field calculations have usually ignored the odd-parity components of the crystal field and that these components may enter calculations in the form $\langle g|V_{cr}^{u}|u\rangle\langle u|V_{cr}^{u}|g'\rangle/\Delta$, adding to terms such as $\langle g|V_{cr}^{g}|g'\rangle$. The electric field effects are simply accounted for by terms of the form $\langle g|V_{cr}^{u}|u\rangle\langle u|eEz|g'\rangle/\Delta$. Artman and Murphy successfully accounted for the magnitude of the D term and for the longitudinal electric field effects in ruby by the inclusion of such terms in an internally self-consistent way, but the values which must be assumed for their adjustable parameters are somewhat unreasonable. First, it was necessary to assume the one-electron spin-orbit parameter ζ for a one-electron excited odd state to be some ten times ζ for a $3d$ electron, whereas the Cr^{3+} free ion spectrum[25] shows that ζ for the $4p$ state is only about three times that for $3d$ state. This reduces the calculated effects by an order of magnitude. The $3p$ electrons have a large ζ but also very large energy denominators, and odd ligand orbitals have no spin-orbit interaction on the chromium center. Second, it was necessary to assume matrix elements of eEz to be some four times larger than would be calculated from free-ion wave functions, and this cannot be explained by orbital expansion in the solid. Furthermore, such a model does not give the correct angular variation, i.e., the ratio of the components of the R tensor. It also predicts that the magnetic resonance electric field effect should scale as $D^{1/2}$, and scaling the electric field effect in ruby to MgO:Cr, one predicts an effect much larger than the experimentally determined upper bound set for the effect in MgO:Cr.

It, therefore, seems more appropriate to treat the electric field effect by a method which takes covalent effects into consideration more explicitly. Molecular orbital calculations[26–28] of the ligand field problem have been shown to answer some of the difficulties[29] arising in a purely electrostatic model of the crystal field.

The observed electric field effect in the Cr^{3+} magnetic resonance is a perturbation of the term $D[S_z^2-\frac{1}{3}S(S+1)]$ in the spin Hamiltonian of the optical ground state of the chromium ion. Thus, a theory for the electric field effect should follow naturally from theory for the ground-state splitting. The $^4A(t_2^3)$ optical ground state is shifted in energy by the spin-orbit interaction energy $\lambda\mathbf{L}\cdot\mathbf{S}$ through the perturbation expression

$$W(^4A)=\sum_n \frac{\langle ^4A|\lambda\mathbf{L}\cdot\mathbf{S}|n\rangle\langle n|\lambda\mathbf{L}\cdot\mathbf{S}|^4A\rangle}{W(^4A)-W(n)}. \quad (9)$$

The intermediate states n include the $^4T_2(t_2^3)$ state and several $^2T_2$ states. The splitting of the ground state arises from an anisotropy in this expression with respect to the orientation of S. In previous calculations[21–24] this anisotropy is attributed to a trigonal crystal field splitting of the $^4T_2$ levels, and this enters Eq. (9) through the energy denominators. Such calculations on chromium in ruby showed that if the optically excited states were located by fitting the optical spectrum, the calculated ground-state splitting was much too small and of the wrong sign as compared to experiment.

It was suggested[22,30,31] that the anisotropy in Eq. (9) would be increased by making the spin-orbit interaction anisotropic through the effects of covalent bonding.

Lohr[28] has shown this to be the case by performing a semiempirical molecular orbital calculation on the complex CrO_6^{-9} with coordinates derived from the Al_2O_3 lattice. Matrix elements of the spin-orbit interaction were evaluated between the resulting molecular orbitals, which are linear combinations of atomic orbitals. The anisotropy in the spin-orbit interaction arises because of differences in the amount of ligand admixture to each of the predominantly $3d$ molecular orbitals. In spite of the use of the molecular orbital formulation, the crystal is still basically ionic, the coefficients of ligand orbital in the predominatly $3d$ molecular orbitals being of the order 0.05. Formally, the anisotropy in the matrix elements of L is transferred[28] to an anisotropy in the spin-orbit parameter λ.

The ground-state splitting parameter D may then be shown[32,33] to be given by

$$D=4[(\lambda_z')^2-(\lambda_x')^2]\{[W(^4A)-W(^4T_2,t_2^2e)]^{-1}-[W(^4A)-W(^2T_2,t_2^2e)]^{-1}\}-3[\lambda_z^2-\lambda_x^2][W(^4A)-W(^2T_2,t_2^3)]^{-1}, \quad (10)$$

where the quadratic expressions in λ and λ' are given by the formulas

$$4\lambda_i'\lambda_j'=\lambda^2\textstyle\sum_{\alpha,\beta}\langle e\alpha|l_i|t_2\beta\rangle\langle t_2\beta|l_j|e\alpha\rangle, \quad (11)$$

$$\lambda_i\lambda_j=\lambda^2\textstyle\sum_{\beta>\gamma}\langle t_2\beta|l_i|t_2\gamma\rangle\langle t_2\gamma|l_j|t_2\beta\rangle. \quad (12)$$

The matrix elements in Eqs. (11) and (12) are evaluated between the one-electron orbit-only molecular orbital wave functions $t_2\alpha$, $t_2\beta$, $t_2\gamma$, $e\alpha$, and $e\beta$. The indices ij run over x, y, and z. In trigonal symmetry, these sums are zero unless $i=j$. The spin-orbit parameter was taken as $\lambda=70$ cm^{-1}, a reduction from the free ion value

[21] J. H. Van Vleck, J. Chem. Phys. **7**, 61, 72 (1939); R. Finkelstein and J. H. Van Vleck, *ibid.* **8**, 787, 790 (1940).
[22] S. Sugano and Y. Tanabe, J. Phys. Soc. Japan **13**, 880 (1958).
[23] D. S. McClure, J. Chem. Phys. **36**, 2757 (1962).
[24] S. Sugano and M. Peter, Phys. Rev. **122**, 381 (1961).
[25] C. E. Moore, *Atomic Energy Levels*, National Bureau of Standards Circular No. 467 (U. S. Government Printing Office, Washington, D. C., 19).
[26] J. H. Van Vleck, J. Chem. Phys. **3**, 803 (1935).
[27] Y. Tanabe and S. Sugano, J. Phys. Soc. Japan **11**, 864 (1956) (III); S. Sugano, Suppl. J. Appl. Phys. **33**, 303 (1962), and references therein.
[28] L. L. Lohr, Jr., and W. N. Lipscomb, J. Chem. Phys. **38**, 1607 (1963).
[29] W. H. Kleiner, J. Chem. Phys. **20**, 1784 (1952).
[30] R. Lacroix, Comp. Rend. **252**, 1768 (1961).
[31] H. Kamimura, Phys. Rev. **128**, 1077 (1962).
[32] Y. Tanabe and H. Kamimura, J. Phys. Soc. Japan **13**, 394 (1958) (IV); Y. Tanabe, Suppl. Progr. Theoret. Phys. (Kyoto) **14**, 17 (1960).
[33] W. A. Runciman and K. A. Schroeder, Proc. Roy. Soc. (London) **A265**, 489 (1962).

of 90 cm^{-1}. This reduction is probably due to a moderate expansion of the chromium wave functions in the solid[34] rather than to a reduction in the angular momentum matrix elements.[35–37]

The electric field effect associated with the ionic polarization of the crystal lattice arises in this formulation because the change in the coordinates of the CrO_6^{-9} complex alters the molecular orbital mixing of the chromium $3d$-atomic orbitals and the ligand orbitals. This alters the spin-orbit anisotropy. The ionic displacements produced by an electric field were not calculated from first principles, but deduced[38–40] from the observed values of the dielectric constant and optical index of refraction.[41] The appropriate internal effective field to be used in calculating polarizations in an ionic solid is taken[40,42,43] to be of the simple Lorentz form for cubic crystals, even though the sites are not cubic.

$$\mathbf{E}_{\text{eff}}=\mathbf{E}+\tfrac{4}{3}\pi\mathbf{P}. \tag{13}$$

This is in contrast to the case of delocalized electrons, where the effective field is better taken[42–45] to be the macroscopic field. The ionic polarization is given by the equation

$$e^*N_0\delta\mathbf{x}=\mathbf{P}_{\text{ion}}=\mathbf{P}-\mathbf{P}_{\text{el}}=\frac{3(\epsilon-n^2)}{4\pi(n^2+2)}\mathbf{E}. \tag{14}$$

The effective charge e^* was taken[40,46] equal to 0.8 times the ionic charge. The perturbation of D due to the ionic displacement $\delta\mathbf{x}$ thus determined was calculated simply by repeating the entire molecular orbital calculations with displaced ionic coordinates. The effect of the displaced coordinates enters in calculating the values of the quadratic expressions in Eqs. (11) and (12). For a displacement of the chromium ion along the c axis with respect to the surrounding oxygen ions, a slightly different value of D results. This change $\delta D=\frac{3}{2}R_{333}E_z$ is the longitudinal electric field effect. This is the only nonvanishing term if trigonal symmetry is preserved. For displacements of the chromium ion in the x and y directions, the transverse and skew components of the R tensor are determined in a similar manner. One replaces the expressions $(\lambda'_z)^2-(\lambda'_x)^2$ or $\lambda_z^2-\lambda_x^2$ in Eq. (10) by the functions of λ or λ' tabulated in Table II. The quadratic expressions given in Table II are to be evaluated using Eqs. (11) and (12) in which the molecular orbitals are calculated with the chromium coordinate displaced by an amount corresponding to a unit electric field in the appropriate direction.

TABLE II. Quadratic expressions in λ to be used in Eq. (10) in place of $\lambda_z^2-\lambda_x^2$ in calculating transverse and skew components of the R tensor.

Displacement along	x	y	z
$R_{111}(\lambda)$	$\frac{1}{2}(\lambda_x^2-\lambda_y^2)$		
$R_{222}(\lambda)$		$-\frac{1}{2}(\lambda_x^2-\lambda_y^2)$	
$R_{123}(\lambda)$	$2\lambda_y\lambda_z$		
$R_{113}(\lambda)$	$2\lambda_x\lambda_z$		
$R_{333}(\lambda)(=\frac{2}{3}\delta D/E)$			$\frac{2}{3}(\lambda_x^2-\lambda_x^2)$
$R_{112}(\lambda)(=-2R_{222})$	$2\lambda_x\lambda_y$		
$R_{212}(\lambda)(=-2R_{111})$		$2\lambda_x\lambda_y$	
$R_{223}(\lambda)(=R_{113})$		$2\lambda_y\lambda_z$	
$R_{213}(\lambda)(=-R_{123})$		$2\lambda_x\lambda_z$	

In order to calculate the electronic effect, it was necessary to evaluate the perturbation $eE_{\text{eff}}z$ between the molecular orbitals calculated with fixed coordinates. It proved more convenient to use the atomic orbitals as a basis set, but to include a crystal field of such a magnitude as to produce the mixing of the atomic orbitals observed in the molecular orbitals. The additional mixing of the orbitals under the influence of the applied field is given by $\langle g|eE_{\text{eff}}z|u\rangle/\Delta$. This additional mixing alters the anisotropy of the spin-orbit interaction and, hence, alters the ground-state splitting. The appropriate effective field in this problem is $\mathbf{E}_{\text{eff}}=(\epsilon+2)\mathbf{E}/3$, assumed identical for all atoms.[47] Taking the electric field along the c axis yielded $\delta D=-3$ Mc/sec for 10^5 V/cm as compared to a calculated ionic effect of $D=+23$ Mc/sec. This calculation is the direct effect of the applied field on the spectrum in mixing the atomic orbitals. These calculations also yielded the electronic polarization of each of the ions and, hence, the index of refraction to be $n^2-1=3.8$. The major contribution comes from the oxygen ion, which means that a comparison with experimental index of refraction for Al_2O_3, $n^2-1=2.1$, shows the validity but relatively poor accuracy of the calculation. There is, however, also an indirect electronic effect, which arises from the fact that the two ions polarize their electron clouds by different amounts and that this relative displacement alters the overlap interaction between the ions. The effect of this electronic motion of the two ions on the spectrum was calculated simply by applying the displaced coordinate results mentioned earlier. This resulted in a total electronic effect of $+3$ Mc/sec. As can be seen, the ionic effect dominates the electronic effect, even allowing for

[34] W. Marshall and R. Stuart, Phys. Rev. **123**, 2048 (1961).
[35] K. W. H. Stevens, Proc. Roy. Soc. (London) **A219**, 542 (1953).
[36] J. Owen, Proc. Roy. Soc. (London) **A227**, 183 (1955).
[37] S. Koide and M. H. L. Price, Phil. Mag. **3**, 607 (1958).
[38] H. Fröhlich, *Theory of Dielectrics* (Oxford University Press, New York, 1949).
[39] C. J. F. Böttcher, *Theory of Electric Polarisation* (Elsevier Publishing Company, Inc., Amsterdam, 1952).
[40] B. Szigeti, Trans. Faraday Soc. **45**, 155 (1949).
[41] *Dielectric Materials and Applications*, edited by A. R. Von Hippel (John Wiley & Sons, Inc., New York, 1954).
[42] S. L. Adler, Phys. Rev. **126**, 413 (1962).
[43] N. Wiser, Phys. Rev. **129**, 62 (1963).
[44] N. Bloembergen, in Proceedings of the Conference on Electric and Magnetic Resonance (Colloque Ampere), Eindhoven, Netherlands, 1962 (to be published).
[45] M. H. Brodsky and E. Burstein, Bull. Am. Phys. Soc. **7**, 214 (1962).
[46] G. O. Jones, D. H. Martin, P. A. Mower, and C. H. Perry, Proc. Roy. Soc. (London) **A261**, 10 (1961).
[47] J. R. Tessman, A. H. Kahn, and W. Shockley, Phys. Rev. **92**, 890 (1953).

the fact that the electronic effect was only crudely evaluated. For this reason, the transverse and skew electronic effects were ignored.

The agreement of the calculated ionic electric field effect with the experimental total electric field effect is better than could be expected, the only significant discrepancy being R_{123}. (See Table III) The electronic effect probably adds 5 to 10% to these values. Note that all calculated signs are in agreement with experiment, both for D and for the components of the R tensor.

TABLE III. Calculated values for the components of the R tensor for the ionic electric field effect and experimental values for the total electric field effect, in Mc/sec per kV/cm except as noted.

	Calculated (ionic effect) CrO_6^{-9}	$Al_4CrO_6^{3+}$	Experimental (total effect)
R_{111}	−0.017	−0.017	−0.020
R_{222}	0.053	0.049	0.073
$R_{333}(=\frac{2}{3}\delta D/E)$	0.154	0.160	0.179
R_{123}	0.008	0.010	0.04
R_{113}	0.092	0.101	0.09
D(Gc/sec)	−11.1	−10.8	−5.4

In an attempt to get better agreement with experiment, the molecular orbitals were extended to include the four next-nearest neighbor aluminum atoms. In general, there is little change in the results, although agreement on R_{123} is slightly improved. Note that R_{123} would be zero in C_{3v} symmetry. The fact that R_{123} is experimentally larger than calculated using Al_2O_3 coordinates may be an indication that the insertion of the Cr^{3+} ion in the lattice in place of the somewhat smaller Al^{3+} ion distorts the local C_3 symmetry further away from C_{3v} symmetry.

In the calculation which included aluminum ions, it was necessary to adjust the oxygen-aluminum interaction by adjusting the diagonal elements of the aluminum atomic orbitals in the effective Hamiltonian. The contact hyperfine interaction of the predominantly $3d$ molecular orbitals on the aluminum nuclei is given by

$$\mathcal{H}=\langle A\rangle \mathbf{I}\cdot\mathbf{S}, \tag{15}$$

where

$$A=\frac{8\pi}{3}g\beta\frac{\mu}{I}\delta(r). \tag{16}$$

If the density of the $3s$ aluminum atomic orbital at the aluminum nucleus is taken[28] as 16×10^{24}/cc, $\langle\delta(r)\rangle$ is simply this value times the square of the $3s$ coefficient in the predominantly $3d$ molecular orbital. With a suitable aluminum-oxygen interaction, values of A were calculated as shown in Table IV. The general agreement with the values obtained in an ENDOR experiment[48] shows that the aluminum-oxygen interaction was adjusted to a reasonable value in the calculations. A possible electric field shift in the ENDOR spectrum was also calculated. The relative change in A caused by the displacement in a field of 10^5 volts/cm is shown in Table IV.

TABLE IV. Calculated and experimental values of the contact hyperfine constant A for predominantly $3d$ molecular orbitals on the next-nearest neighbor aluminum nuclei (in Mc/sec) and the calculated electric field induced fractional change in A.

Field of 10^5 V/cm along axis	A (calc)	A (expt)	x	y	z
Al in plane of Cr	3.8	3.24	−0.00072	0.00012	−0.00004
	3.8	3.24	0.00048	0.00058	−0.00004
	3.8	3.24	0.00026	−0.00058	−0.00004
Al on axis of Cr	2.8	0.68	···	···	−0.00064

The dielectric constants[41] of Al_2O_3 were used to determine the displacement of the chromium in the Al_2O_3 lattice. If the dielectric constants[49] of Cr_2O_3 (having the same structure but different cell parameters) are used, the calculated electric field effects would increase by 86 and 18% perpendicular and parallel to the c axis, respectively. There seems no strong reason for choosing either data to describe the polarizability of the chromium impurity in the Al_2O_3 lattice, although it seems more reasonable to use the Al_2O_3 constants.

The chromium defect site in MgO was treated by the same semiempirical molecular orbital method as was outlined for ruby. All parameters were kept the same as in the ruby calculation except for the coordinates of the ions in the complex. The geometry of the complex was taken to be that of the magnesium site but with the complex stretched 0.1 Å along the chrom-oxygen-vacancy axis to simulate a possible tetragonal distortion of the octahedron, which might exist due to the charge compensating vacancy on the far side of one oxygen. The value of the cubic optical splitting was successfully calculated by this method as it was for ruby. The calculated ground-state splitting $2D$ was an order of magnitude smaller than that observed. Apparently the ground-state splitting is due almost entirely to just the electrostatic field from the charged vacancy.

A purely electrostatic calculation of the matrix elements of the field from a charge at the position of the vacancy yields a value of D which is 2.5 times smaller than that observed, but the larger value of D may originate from the effects of configuration mixing, as has been pointed out for ruby.[24] Using this electrostatic model, the predicted electric field effects for 10^5 V/cm are $\delta D=0.3$ Mc/sec and 0.6 Mc/sec for the ionic and electronic effects, respectively, and the total effect is conveniently smaller than the experimental upper bound of 1.0 Mc/sec. Effects of both odd and even components of the electrostatic field were included, the contribution of the odd component to D being some 25% of the total. The formalism of Artman and Murphy[19] was used but with more reasonable values of

[48] N. Laurence, E. C. McIrvine, and J. Lamb, J. Phys. Chem. Solids 23, 515 (1962).

[49] P. H. Fang and W. S. Brower, Phys. Rev. 129, 1561 (1963).

the parameters. The spin-orbit interaction in the excited state was ignored, and matrix elements of the electrostatic field from the point change at the vacancy site were taken to have the values obtained from free ion wave functions[28] rather than these values multiplied by some factor of the order 4.

IV. CONCLUSION

The use of the electric field effect in paramagnetic resonance gives very detailed information on the local symmetry of the paramagnetic sites. if these sites are not inversion centers. The electric field effect extends the usefulness of the paramagnetic resonance technique in probing local symmetries in solids, by giving information on the odd-parity components of the effective crystalline field.

The molecular orbital calculations of the induced electric shifts have added to the evidence for the inadequacy of the point-charge crystal field theory[50] and to the evidence for the validity of the molecular orbital approach[26–28] to the crystal field problem. The anisotropy of the electric shifts cannot even be accounted for by the more generalized crystal field theory with several adjustable parameters.[19,20,22] The ground-state splitting and electric field effect on the ground-state splitting for chromium in ruby can be explained satisfactorily when anisotropy of the spin-orbit interaction is explicitly taken into account. This anisotropy is shown to be due to covalent effects.

ACKNOWLEDGMENTS

The assistance of L. L. Lohr, Jr., in the theoretical part of this work is gratefully acknowledged. The semiempirical molecular orbital procedure used is his, and he has programmed all of the computer runs reported. We thank Dr. J. O. Artman and Dr. M. Weger for preprints of their articles. Conversations with F. A. Collins have been very fruitful.

APPENDIX. ON POSSIBLE EFFECTS OF A PERMANENT ELECTRIC DIPOLE MOMENT

The implications of the existence of a permanent electric dipole moment for the electron in paramagnetic resonance, have been treated by Sachs and Schwebel.[51] The existence of the electronic dipole moment, which would require the nonconservation of both parity and time-reversal symmetry, would cause a lifting of the Kramers degeneracy,[52] and, hence, a shift in paramagnetic resonance frequencies under the application of an electric field or in the presence of a crystalline field of odd parity.

The experimental electric field induced shifts in paramagnetic resonance of Cr^{3+} in Al_2O_3 described in this paper are proportional to the product of the applied electric field and the internal crystal field component of odd parity. They have nothing to do with the existence of permanent dipoles. By reversing the direction of the applied electric and magnetic fields in our experiments, it is possible to separate the ordinary electric field shift from a possible shift produced by an electronic dipole moment. Verification of the Kramers degeneracy for the spin doublets of the orbital ground state of Cr^{3+} in Al_2O_3 provided an experimental upper bound on the intrinsic electric dipole moment of the electron to the limit of the experimental accuracy.

Assume the electron to have an intrinsic electric dipole moment $\mathbf{P}=2\xi\beta\mathbf{s}$. Then the Hamiltonian for the electron will contain a term

$$\mathcal{H}'=-2\xi\beta\mathbf{s}\cdot(\nabla\phi). \tag{17}$$

The parameter ξ is a pseudoscalar. This term will lift the degeneracy between the $\pm\frac{1}{2}$ states and between the $\pm\frac{3}{2}$ states. In the absence of the spin-orbit interaction, the average electric field acting on a bound electron in a solid $\langle\nabla\phi\rangle$ must be zero. If an external electric field or a crystalline field of odd parity is present, it is exactly cancelled by a displacement of the bound electronic orbital with respect to all other charges. The total average force on the bound electron is zero. In the presence of the spin-orbit interaction, part of the net force may be of magnetic origin, and the average electric field need not be exactly zero. The electric field to be used in Eq. (17) is approximately the field applied to the atom multiplied by a reduction factor of the order λ/Δ. Sachs and Schwebel show that the perturbation of the spin energy levels by this average electric field acting on the permanent electric dipole moment is given by an expression of the form,

$$\begin{aligned}\Delta W=2\xi\beta k(W_n-W_{n'})^{-1}&\\ \times\{&[\langle n|\mathbf{s}\cdot\nabla\times[(\nabla\phi^g)\times\nabla]|n'\rangle\\ &-\langle n|\mathbf{s}\cdot[(\nabla\phi^g)\times\nabla]\times\nabla|n'\rangle]\langle n'|e\phi^u|n\rangle\\ &+\text{transpose}\},\end{aligned} \tag{18}$$

with $k=(\hbar/2mc)^2$. The second term, arising from a commutator expression, has apparently been omitted by Sachs and Schwebel. For real wave functions the addition of the transpose is equivalent to multiplication by 2. The even- and odd-parity components of a crystalline field or an applied field are represented by the potentials ϕ^g and ϕ^u, respectively. If the one-electron spin-orbit energy is written in the usual way, $V_{so}=-iek2\mathbf{s}\cdot(\Delta\phi)\times\nabla=\zeta\mathbf{l}\cdot\mathbf{s}$, one obtains

$$\begin{aligned}\Delta W=2\xi\beta(W_n-W_{n'})^{-1}\{&\langle n|\mathbf{s}\cdot\nabla\times i\zeta\mathbf{l}|n'\rangle\\ &-\langle n|\mathbf{s}\cdot i\zeta\mathbf{l}\times\nabla|n'\rangle\}\langle n'|\phi^u|n\rangle.\end{aligned} \tag{19}$$

[50] W. Low, *Paramagnetic Resonance in Solids* (Academic Press Inc., New York, 1960).
[51] M. Sachs and S. Schwebel, Ann. Phys. (N.Y.) 8, 475 (1959); M. Sachs, *ibid.* 6, 244 (1959).
[52] H. A. Kramers, Proc. Acad. Sci. Amsterdam 33, 959 (1930).

Define the tensor $\mathbf{A}$ by the equation

$$\langle\nabla\phi^u+\mathbf{E}\rangle\cdot\mathbf{A}=-e\sum_n\{\langle 3d_n|\nabla\times i\mathbf{l}|u\rangle(\zeta_u/3)-\langle 3d_n|i\mathbf{l}\times\nabla|u\rangle(\zeta_{3d}/3\}\times\langle u|e\phi^u+eEr|3d_n\rangle(W_{3d}-W_u)^{-1},\quad(20)$$

where $\mathbf{E}$ is a possible applied electric field and ϕ^u is the odd-parity component of the crystal field. The tensor $\mathbf{A}$ has only diagonal elements nonzero, and one has $A_{xx}=A_{yy}\neq A_{zz}$ in the C_3 site symmetry of ruby.

Then

$$\Delta W=-2\xi\beta\mathbf{S}\cdot\mathbf{A}\cdot\langle\nabla\phi^u+\mathbf{E}\rangle.\quad(21)$$

The component of the tensor A_{zz} was numerically evaluated as $A_{zz}=1.15\times10^{-3}$ with a probable error of a factor of 2 by the use of Eq. (20). Major contributions come when the odd-state u is a $3p$ and $4p$ or $4f$ state. Other chromium states have larger energy denominators and/or smaller matrix elements to the ground state. Odd-ligand molecular orbitals made up of oxygen atomic orbitals also have small matrix elements for this perturbation, although they dominate in producing the ordinary electric field effects. Parameters derived from optical spectra[25] were used in the calculation, and matrix elements of z and ∇ were evaluated using Slater-type wave functions.[28] In calculating the interactions between orbitals only on the chromium, the crystal field was evaluated at the nucleus from a purely electrostatic model; the major odd-parity component is a field along the c or z axis. For the ligand orbital interaction, the effective crystal field was evaluated by the molecular orbital method.

The electric field effects are introduced into the usual spin Hamiltonian describing the spin energy levels of the paramagnetic ion by the addition of the following perturbation terms:

$$\mathcal{H}'=\sum_i\sum_{j\leq k}\tfrac{1}{2}R_{ijk}E_i(S_jS_k+S_kS_j)-\sum_{ij}2\xi\beta A_{ij}S_i\langle\nabla\phi^u+E\rangle_j.\quad(22)$$

The first term represents the ordinary electric field effect described previously, and the second is the dipole-induced effect which lifts the Kramers degeneracy. Browne[53] has attempted to detect the dipole-induced effect experimentally by applying a uniform electric field to a paramagnetic salt. However, the term $\nabla\phi^u$ is much larger than any possible applied electric field if the paramagnetic site lacks inversion symmetry, as is the case in ruby. This fact was taken advantage of in the present work. If the $-\frac{1}{2}\rightarrow\frac{3}{2}$ transition of Cr^{3+} in ruby is observed with the magnetic field along the z or c axis, there should be a shift in frequency given by

$$\delta\nu=h^{-1}\{3R_{zzz}E_z-2\xi\beta A_{zz}\langle\nabla\phi^u\rangle_z\}.\quad(23)$$

The dominant part of $\nabla\phi^u$ is along the c axis. Now for both electric and magnetic fields along the c axis, the four sites in the Al_2O_3 lattice become equivalent in pairs. The members of one pair are related to members of the other pair by inversion. Both terms in Eq. (23) are of opposite sign for one of these pairs of sites as compared to the other pair because $\nabla\phi^u$ changes sign on inversion. $\mathbf{R}$ is proportional to $\Delta\phi^u$, whereas $\mathbf{A}$ is not. Thus, $\delta\nu$ in Eq. (23) produces a splitting of the observed resonance line in ruby since the resonance frequency for the two pairs of sites shifts in opposite directions.

If the direction of the applied magnetic field is reversed, only the second term in Eq. (23) will reverse in sign. Reversal of the magnetic field reverses the direction of the z axis and, hence, the sign of $\mathbf{E}$, and $\mathbf{R}$, and $\Delta\phi^u$. On the other hand, reversing the sign of the applied electric field reverses the sign of only the first term if one assumes that $\nabla\phi^u\gg E$. Thus, on reversal of either the applied electric or the applied magnetic field, the splitting $(=2|\delta\nu|)$ changes by 4 times the second term in Eq. (23). If Δ represents the change on reversal of either the applied electric or magnetic field, one has

$$\Delta(2|\delta\nu|)=8h^{-1}\xi\beta A_{zz}\langle\nabla\phi^u\rangle_z.\quad(24)$$

Any possible additional splitting due to the T-tensor terms would have the same symmetry as the R-tensor terms as far as reversal of sign is concerned. Hence, possible effects of a T-tensor term may be lumped with the first term of Eq. (22) at fixed field and frequency. One may inquire as to why any electric field was applied, thereby introducing the complication of the ordinary electric field effect. The electric dipole splitting by itself must be assumed to be much smaller than one linewidth, and hence, the observed additional broadening of the line produced by the dipole effect would be proportional to the square of the effect. Also, there would be no way to "turn off" the induced broadening. The ordinary electric field is used to initially split the line, in which case any additional splitting arising from the dipole effect is directly observable.

In this work the procedure was to observe the electrically induced line splitting for four cases: (1) electric and magnetic fields normal, (2) magnetic field reversed, electric field normal, (3) both fields reversed, and (4) electric field reversed, magnetic field normal. The difference between the line splittings for the second and fourth cases, on the one hand, and the first and third cases, on the other hand, is $\Delta(2\delta\nu)$. Experimentally, this quantity was found to be (0.025 ± 0.125) G or (0.07 ± 0.35) Mc/sec. The uncertainty quoted is based on the standard deviation of the results of eight runs. In Eq. (24) one has $A_{zz}=1.15\times10^{-3}$ and from a purely electrostatic model $\nabla\phi^u=3.6\times10^8$ V/cm, which yields $|\xi|=(0.5\pm2.3)\times10^{-5}$. (Taking into account only nearest neighbor oxygen ions gives $\nabla\phi^u=6\times10^8$ V/cm, but a lattice sum[23] gives the value used.) Remembering the possible uncertainty in A_{zz} of a factor of 2, it is possible to say only that $|\xi|$ is probably less than 3.5×10^{-5} and almost certainly less than 7×10^{-5}. The latter corre-

[53] M. E. Browne, Phys. Rev. **121**, 1699 (1961).

sponds to a dipole moment of 1.4×10^{-15} cm times e. This upper bound on the electric dipole moment of the electron is three times lower than the bound set by Nelson *et al.*,[54] but not as good as the bound of 4×10^{-16} cm times e set by Wilkinson *et al.*[55] or the bound of 10^{-15} set by Goldemberg and Torizuka.[56]

In view of the molecular orbital theory of crystal fields developed previously, one may question the use of the simple electrostatic crystal field theory in calculating the dipole effect. Unfortunately, while the semiempirical molecular orbital theory is very good in treating the chrome-ligand interactions, it is unsatisfactory in treating the interactions between the various electron orbitals on the chromium ion, and it is just these interactions which are dominant in calculating the dipole effect. The electrostatic model used in evaluating Eq. (20) is probably conservative in estimating the value of $\nabla\phi^u$.

The experimental limitations which prevented a better upper bound from being set on the electric dipole moment of the electron by this method arise mainly from instrumental instabilities over the period of a run. More fundamental, however, is the limitation that this measurement depends on the calculation of effective crystalline fields in a solid, a problem whose solution is still beset with considerable uncertainty. The approximations used in the calculations here are quite crude, but a better calculation must await better wave functions and energy levels for excited states of an atom in a solid, and a better theory of the crystalline field.

[54] D. F. Nelson, A. A. Schupp, R. W. Pidd, and H. R. Crane, Phys. Rev. Letters **2**, 492 (1959).
[55] D. T. Wilkinson and H. R. Crane, Phys. Rev. **130**, 852 (1963).
[56] J. Goldemberg and Y. Torizuka, Phys. Rev. **129**, 2580 (1963).

PHYSICAL REVIEW VOLUME 131, NUMBER 5 1 SEPTEMBER 1963

Theory of the Magnetic and Optical Properties of Cr_2O_3†

G. W. PRATT, JR., AND P. T. BAILEY
Materials Theory Group, Department of Electrical Engineering, Massachusetts Institute of Technology, Cambridge, Massachusetts

(Received 18 April 1963)

Cr_2O_3 is discussed from the point of view of pairs of Cr ions with strong exchange coupling between members of the pair and subjected to a relatively weak molecular field. This is done using the Oguchi method. The anomalous behavior of the parallel susceptibility above T_N and low-temperature spin-saturation value are explained. If the spin system is assumed to be canted, it is possible to explain the nonzero value of $\chi_{||}$ at 0°K and the resultant optical properties are found to be in good agreement with experiment.

I. INTRODUCTION

THIS study of the magnetic and optical properties of Cr_2O_3 was stimulated by the very interesting high-resolution measurements of the optical absorption of Cr_2O_3 at 4.2°K by Wickersheim.[1] He found that using a spin-Hamiltonian description of an individual Cr^{3+} ion subjected to both a crystal field and an effective magnetic field due to exchange, there appear various discrepancies between the consequences of this model and the experimental results. Since Cr_2O_3 can be thought of as being constructed from a set of parallel chains of atoms with each chain a c axis along which the Cr^{3+} ions are grouped as pairs of Cr^{3+} ions with a relatively large separation between pairs, it seems more natural to use a model which treats the optical properties of a pair of Cr^{3+} ions rather than individual Cr^{3+} ions. In Fig. 1 we show the atomic arrangement along the c axis. Our model consists, then, of a pair of Cr^{3+} ions such as the pair $A-B$ in Fig. 1 with an antiferromagnetic superexchange coupling between these ions. The crystalline environment subjects the pair to a crystal field and an effective magnetic field from exchange interactions with the pair. With this geometric arrangement, the method of Oguchi[2] seems ideal to discuss Cr_2O_3 and this is the scheme used in this analysis.

The results obtained are very satisfactory. Not only can the optical properties be accounted for but the anomalous magnetic properties of Cr_2O_3 can also be explained by the same model. These anomalies are the failure of the parallel magnetic susceptibility $\chi_{||}$ to vanish at 0°K and the failure of $\chi_{||}$ to drop sharply as the temperature increases through the Néel point. Our theory further predicts that the sublattice spin per Cr will not saturate at 0°K to 1.5 but more nearly to 1.3. In addition, we predict that the Cr spins order in some form of canted spins forming spirals. The introduction of canted spins into our model provides an explanation of the low-temperature behavior of $\chi_{||}$ and at the same time improves agreement with the optical anisotropy

† This work was supported in part by the U. S. Office of Naval Research.
[1] K. A. Wickersheim, J. Appl. Phys. **34**, 1224 (1963).
[2] T. Oguchi, Progr. Theoret. Phys. (Kyoto) **13**, 148 (1955).